ingegneria sismica
International Journal of Earthquake Engineering
Anno XLIII - Num. 3 - 2026

Data-driven aero-engine fault diagnosis fusion algorithm optimization and health management strategy

Xiaolong Che[1,2,*], *Min Liu*[3] *and Jiao Li*[3]

[1] School of Aerospace Engineering, Xiamen University, Xiamen, 361102, Fujian, China
[2] Service Support Department, AECC South Industry Co., Ltd., Zhuzhou, 412002, Hunan, China
[3] Optoelectronic Technology Branch, AECC South Industry Co., Ltd., Zhuzhou,412002, Hunan, China

SUMMARY: *A data-driven fault diagnosis fusion algorithm and health management framework was proposed to solve the problems of asynchronism, feature redundancy and instability of weak fault recognition in multi-source monitoring data of aero-engine. Method The method takes 21 types of sensor variables and three types of working condition parameters as input. After abnormal correction, normalization, and sliding window coding, the channel sensitivity prior, adaptive weight allocation, and error feedback correction mechanism are introduced to form a fusion feature for fault classification, diagnostic confidence calculation, and health state assessment. The experimental results show that the model Accuracy is 96.37%, F1-score is 95.74%, AUC is 98.21%, and the average inference time is 19.8 ms. Compared with Transformer, the F1-score is improved by 2.55 percentage points and the inference time is reduced by 8.1 ms. Ablation results show that the adaptive weight and error correction contribute significantly to the performance of the model, which can support the stable transformation of fault identification results to maintenance strategy output.*

KEYWORDS: *aero-engine; Fault diagnosis; Feature fusion; Health management*

1 Introduction

Aero-engine runs in high temperature, high pressure, high speed and strong vibration environment for a long time, and there are complex coupling relationships between compressor, combustion chamber, turbine, bearing and accessory systems. The engine monitoring system can continuously collect multi-source data such as speed, exhaust gas temperature, fuel flow, vibration, pressure, oil temperature and component efficiency. However, the signal amplitude of the early fault is weak and the propagation path is long, which is easy to be masked by the switching of operating conditions and sensing noise. Traditional threshold alarm and single sensor diagnosis methods are difficult to fully express the fault evolution process, and multi-sensor fusion has become an important direction of intelligent fault diagnosis of rotating machinery [1].

In recent years, machine learning and deep learning methods have been widely used in aero-engine fault diagnosis. Related studies have shown that convolutional neural network, recurrent neural network, attention mechanism and deep fusion model can extract nonlinear

*Chexiaolong88314@163.com
https://doi.org/10.65102/is20261277 Published: 10 June, 2026

features from complex monitoring data and improve fault recognition accuracy [2-4]. In the predictive maintenance task of turbofan engines, deep learning methods have been used for remaining useful life estimation, degradation trend identification and operation state classification [5]. Research on aero-engine health management has also gradually shifted from off-line fault interpretation to data-driven condition perception, risk assessment and closed-loop maintenance decision-making [6].

The existing methods still face the problems of multi-source data asynchronism, feature redundancy, working condition disturbance and insufficient model generalization in engineering applications. The sampling frequency, response sensitivity and fault correlation of different sensors are different, and direct splicing features are easy to cause noise accumulation. The fixed-weight fusion is difficult to adapt to the state changes of the engine from starting, climbing, cruising to descending stages. The single classification output lacks confidence interpretation, which is difficult to support maintenance strategy generation. Complex system fault diagnosis needs to take into account deep feature learning, model stability and online reasoning efficiency [7], and intelligent maintenance strategies also need to transform diagnosis results into executable health management instructions [8].

Based on the above problems, this paper constructs a data-driven aero-engine fault diagnosis fusion algorithm optimization and health management method. The model takes multi-source monitoring data as input, completes outlier processing, time series window segmentation, feature coding and adaptive weight allocation. The dynamic weight update and error correction mechanism were introduced in the fusion layer to enhance the weak fault feature expression. In the diagnosis layer, the fault classification, confidence calculation and health status assessment modules are constructed. In the output layer, the maintenance level, the overhaul window and the risk warning strategy are formed. The method forms a closed loop through data processing, fusion algorithm, diagnosis model and experimental verification, and provides a reproducible computational framework for aeroengine condition recognition and health management.

2 Related Research

Multi-source monitoring data fusion is an important basis for aero-engine fault diagnosis research. In the process of engine operation, signals such as temperature, pressure, speed, vibration, fuel flow, and oil parameters jointly reflect the state of compressor, combustor, turbine, bearing and control system. However, different sensors have differences in sampling frequency, response time delay, noise level and fault sensitive area. Zhang et al. [9] proposed a multi-modal feature fusion method to show that multi-source signals can enhance the expression of weak fault information after entering the unified feature space. Li et al. [10] summarized multimodal deep learning fault diagnosis and pointed out that feature-level fusion, decision-level fusion and hybrid fusion can adapt to different data structures. Zhou et al. [11] applied multi-scale feature fusion to aero-engine degradation prediction, which provided a method reference for multi-condition state recognition.

The effectiveness of the data fusion method depends on the quality of the features, the channel weights, and the adaptability of the model to changes in operating conditions. Garcia et al. [12] analyzed the data fusion strategy in industrial fault diagnosis and emphasized that sensor credibility and feature correlation would affect the fusion results. Yin et al. [13] constructed a multi-source information fusion method for aero-engine fault diagnosis, and verified the effect of multi-channel monitoring data on fault mode differentiation. Existing research shows that simple stitching is easy to introduce redundant information and noise

interference, and fixed weight is difficult to adapt to complex operation stages such as starting, climbing, cruising and descent. The fusion algorithm needs to have the ability of dynamic weight adjustment, abnormal feature suppression and cross-working condition adaptation.

In terms of fault diagnosis models, deep learning methods have shifted from single network structure to hybrid models. Wu et al. [14] used CNN-BiLSTM model to combine local feature extraction and timing dependence modeling for engine monitoring sequence recognition. Du et al. [15] combined the LSTM autoencoder with the attention mechanism for anomaly detection and key time slice localization. Zhou et al. [16] proposed a multi-head attention fault diagnosis method to extract multi-scale correlation information through different attention subspaces. Zhang and Yang[17] constructed a convolutional Transformer model to combine convolutional features with global dependency modeling to improve the ability of long sequence fault feature aggregation.

The aeroengine diagnostic model also needs to meet the real-time and online adaptation requirements. Liu et al. [18] proposed a real-time fault diagnosis framework, focusing on model inference latency, online deployment and engineering availability. Wang et al. [19] applied reinforcement learning to adaptive fault diagnosis, so that the model could adjust the diagnosis strategy according to feedback. Chen et al. [20] studied adaptive feature selection and weight allocation methods to provide support for redundant feature compression and effective feature enhancement. Garcia and Ruiz[21] proposed an online learning diagnosis system, which can update the model parameters under the continuous input of new samples, and is suitable for dealing with the drift problem of engine conditions in long-term service.

Health management research focuses on the transformation of diagnostic results into maintenance strategies. Kim and Lee[22] constructed an adaptive health monitoring method to incorporate state estimation, model optimization, and health evaluation into a unified process. Goebel and Saxena[23] carried out research on the remaining life prediction of aeroengine, indicating that the fault diagnosis results need to be further transformed into life estimation, risk level and maintenance window. Kim and Lee[24] studied health state estimation and maintenance decision to provide reference for the design of engine health management module. To further sort out the correspondence between different research directions and the tasks of this paper, Table 1 summarizes the related results.

Table 1: Summary of related studies

Research Direction	Representative Literature	Main Methods	Support for This Paper
Multi-source feature fusion	[9-13]	Multimodal fusion, multi-scale feature fusion, multi-source information fusion	Supports the design of monitoring data encoding, feature interaction and weight allocation
Deep diagnostic model	[14-18]	CNN-BiLSTM, LSTM autoencoder, multi-head attention, convolutional Transformer	Supports the fault classification model, temporal feature extraction and real-time diagnostic structure
Adaptive algorithm optimization	[19-21]	Reinforcement learning, adaptive feature selection, online learning	Supports fusion weight updating, error correction and operating condition drift adaptation
Health management decision-making	[22-24]	Health status estimation, remaining useful life prediction, maintenance decision-making	Supports health assessment, risk classification and maintenance strategy output

Existing research has provided methodological support in data fusion, deep diagnosis, adaptive optimization and health management, but there is still a lack of connection between different research directions. Multi-source fusion research pays more attention to feature complementarity and recognition accuracy, and rarely discusses how fusion features enter health status assessment. Most deep diagnosis models take classification accuracy, recall rate and loss convergence as the core indicators, and do not consider the confidence expression of diagnosis results and maintenance availability. Health management research emphasizes life prediction and maintenance decision-making, but its input often depends on the established health indicators, and does not make full use of the dynamic characteristics and error information generated within the fault diagnosis model.

In this paper, a systematic fault diagnosis and health management method for aeroengine is proposed, which integrates multi-source sensor feature adaptive fusion, error correction, diagnostic confidence calculation and health state mapping into a unified computing framework, and realizes the closed-loop processing from original features to executable maintenance strategies. This method effectively improves the recognition ability of weak fault features, enhances the reliability and interpretability of diagnosis results, and supports the application in complex operating environments such as multiple operating conditions, sensor noise and sample distribution drift. Through the dynamic weight adjustment and error feedback mechanism, the fusion layer can give priority to the key channel characteristics, provide accurate input for the health management module, ensure the scientifi - ciality and operability of maintenance strategy generation, and provide a robust technical support for the actual aeroengine intelligent maintenance.

A complete data-driven research route is constructed in this paper to address the problems of condition switching, weak fault submerging and sensor noise in the actual operation scenario of aero-engine. Firstly, multi-source sensor signal synchronization, outlier correction and window segmentation were implemented in the data preprocessing stage to ensure the reliability of model input. Then, the adaptive fusion algorithm and error correction mechanism were used to realize the dynamic optimization of features to improve the diagnostic performance. Then, confidence calculation and health state mapping are introduced into the diagnosis model to convert the fused features into executable maintenance recommendations. Finally, a closed-loop system from feature extraction, fusion optimization, fault recognition to health management strategy output is formed, which provides a clear research basis and technical route guidance for the fusion algorithm optimization and health management module construction in the subsequent chapters.

3 Data-driven optimization of fault diagnosis fusion algorithm

3.1 Feature coding and weight allocation of multi-source monitoring data

Aero-engine operation monitoring data come from multiple sensor channels such as temperature, pressure, speed, vibration, fuel and lubricating oil. The sampling frequency, dimension range, noise level and fault sensitive objects of each channel are not consistent. If the original data is directly input into the fusion model, variables with large amplitude such as pressure and temperature are easy to amplify the gradient contribution, and weak fault features such as vibration impact and oil pressure fluctuation may be weakened. In order to ensure that the subsequent fusion algorithm obtains stable input, it is necessary to complete time synchronization, anomaly correction, scale normalization, window construction and channel weight initialization, so that the multi-source data can be converted into computable,

comparable and fusing time series features.

Suppose that there are M types of sensor channels at time t, the observation value of the m-th type channel is xm(t), the working condition variable is c(t), and the multi-source monitoring vector is expressed as follows.

$$X(t)=[x_1(t),x_2(t),\ldots,x_M(t),c(t)]^T \tag{1}$$

where, X(t) is the multi-source monitoring input at time t; xm(t) is the observation value of the m-th sensor; M is the number of sensor channels; c(t) is the working condition variable, which can be composed of speed level, thrust state or environmental correction.

Abnormal sampling points can change the statistical distribution in a short time window, especially affecting features such as vibration RMS, temperature slope, and pressure fluctuation. Let μm and σm be the historical mean and standard deviation of the m-th channel, $\tilde{x}_m(t)$ be the neighborhood smoothing value, τ be the anomaly threshold, and the corrected observation value is as follows.

$$\tilde{x}_m(t)=\begin{cases} x_m(t), |x_m(t)-\mu_m|\le\tau\sigma_m \\ \bar{x}_m(t), |x_m(t)-\mu_m|>\tau\sigma_m \end{cases} \tag{2}$$

where, $\tilde{x}_m(t)$is the channel value after anomaly correction; μm and σm are used to determine the degree of data offset. $\tilde{x}_m(t)$ is the local neighborhood mean or median filtering result; τ controls the anomaly identification sensitivity.

Different monitoring channels correspond to different fault-sensitive objects, and feature coding needs to preserve component directivity. To clarify the role of each channel in feature coding, Table 2 sorts out the main data sources, coding features and fault sensitive components.

Table 2: Multi-source monitoring data channel and feature coding description table

Data Channel	Main Variables	Encoding Features	Fault-sensitive Components
Temperature channel	Exhaust temperature, lubricating oil temperature	Mean value, slope, fluctuation amplitude	Turbine, combustion chamber, lubrication system
Pressure channel	Compressor outlet pressure, lubricating oil pressure	Peak value, pressure ratio change rate	Compressor, lubricating oil system
Speed channel	High-pressure rotor speed, low-pressure rotor speed	Speed deviation, acceleration response	Rotor system, control system
Vibration channel	Casing vibration, bearing vibration	RMS, kurtosis, frequency band energy	Bearing, rotor imbalance
Fuel channel	Fuel flow, fuel regulation amount	Flow fluctuation, control deviation	Fuel system, combustion chamber

The temperature, pressure and fuel channels mainly describe the thermal performance and control response changes, the vibration channel is more suitable for capturing bearing impact and rotor imbalance, and the oil related variables can supplement the abnormal information of the lubrication system. After anomaly correction, all kinds of variables enter a unified scale

space to avoid dimensional differences affecting fusion weight learning. Normalization is performed as follows:

$$z_m(t)=\frac{\tilde{x}_m(t)-x_m^{min}}{x_m^{max}-x_m^{min}+\varepsilon} \tag{3}$$

where, zm(t) is the MTH channel feature after normalization; x_m^{min} and x_m^{max} are the training set boundary values. ε is the smoothing term, which is used to prevent the denominator from being zero.

Before multi-source monitoring data enters the model, it needs to be transformed from the original sampling sequence into training samples with time continuity. To ensure the reliability of multi-source sensor signals and the quality of model input, the complete process of data preprocessing and time series sample construction is shown in Figure 1.

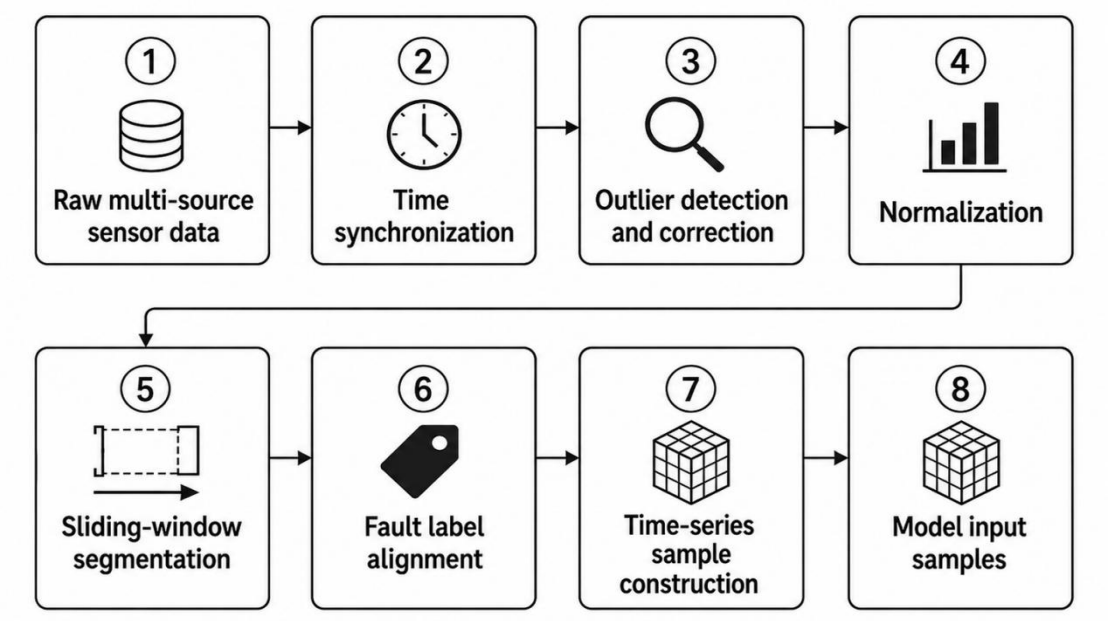

Figure 1: Process of multi-source sensor data preprocessing and time series sample construction

Each step ensures that the original signal can generate standardized training samples for the model to use after synchronization, anomaly correction, normalization and sliding window segmentation.

This processing link aligns sensor signals with different sampling frequencies to a unified time axis, and then preserves continuous segments of fault evolution through a sliding window. Let the window length be L, the step size be s, the normalized multi-channel feature vector be z(t)=[z1(t),z2(t),...,zM(t)], and the ith window sample be:

$$S_i=[z(t_i),z(t_i+s),\ldots,z(t_i+(L-1)s)] \tag{4}$$

where, Si is the ith time series window sample; L is the window length. s is the sliding step size; z(t) is the normalized multi-channel feature vector. Window samples are used to preserve the short-time continuity of engine state changes.

After the construction of window samples, each channel still needs to assign initial

weights according to the fault sensitivity. The response of different sensors to engine faults is not the same, and the temperature, pressure, speed, vibration, fuel and lubricating oil parameters correspond to thermal performance, gas path state, rotor dynamics and lubrication state changes, respectively. The response relationship between sensor channels and fault types can be represented by an association network, as shown in Figure 2.

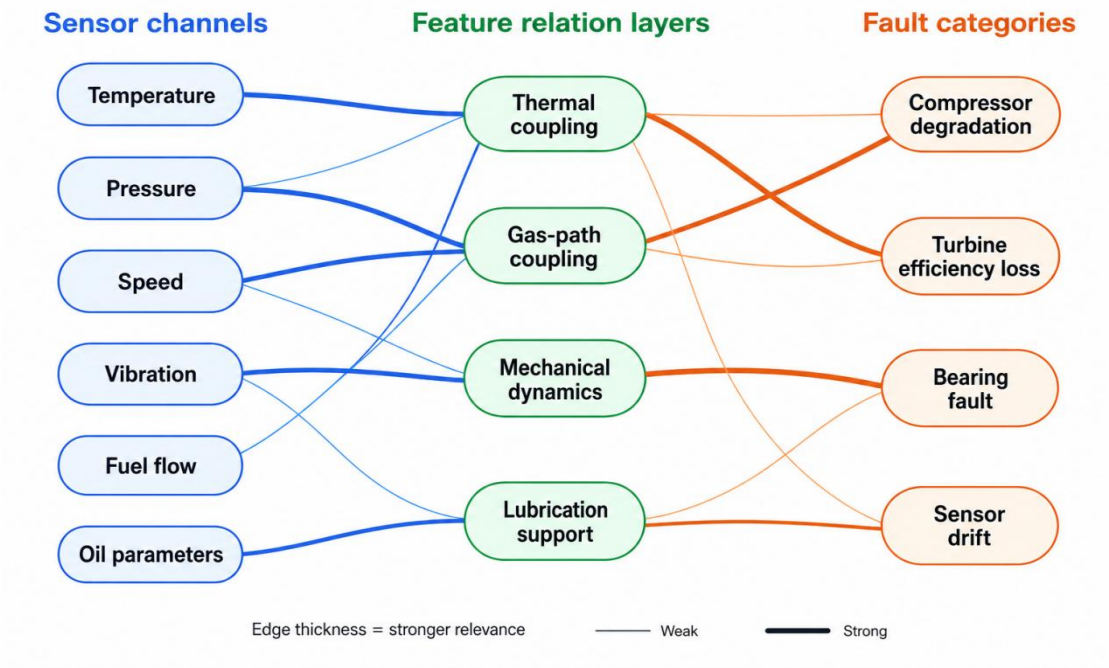

Figure 2: Multi-source sensor feature correlation and fault sensitivity correlation network diagram

In the association network, nodes represent sensor channels and fault categories, and wire thickness represents response strength. The vibration channel is more strongly connected with the bearing anomaly, the pressure and speed channels are more responsive to the compressor degradation, and the temperature and fuel channels are more sensitive to the decrease of turbine efficiency. The oil parameters mainly supplement the identification of lubrication anomaly and sensor drift. This association is used as the initial weight allocation basis, so that the fusion layer can give priority to the channels with stronger fault direcency in the early training stage, and continue to update with the diagnosis error in subsequent iterations.

3.2 Design of adaptive feature fusion algorithm

After the windowing coding of multi-source monitoring features is completed, there are still differences in the contributions of different channels. Temperature, pressure, speed, vibration, fuel and oil parameters are sensitive to different fault types. Fixed splicing will weaken the diagnostic role of critical channels, and static weighting is difficult to adapt to the changes in starting, accelerating, cruising and pushing down conditions. In order to make the fusion process dynamically adjust with the sample state, the algorithm established an adaptive connection among channel coding, timing extraction, weight calculation and feature aggregation.

The adaptive fusion algorithm needs to establish a clear calculation link between multi-channel input, temporal feature coding, weight generation and fusion output. Each module completes feature coding, dynamic weight adjustment and fusion operations in turn to provide high-quality feature input for subsequent diagnosis and health management, as shown

in Figure 3.

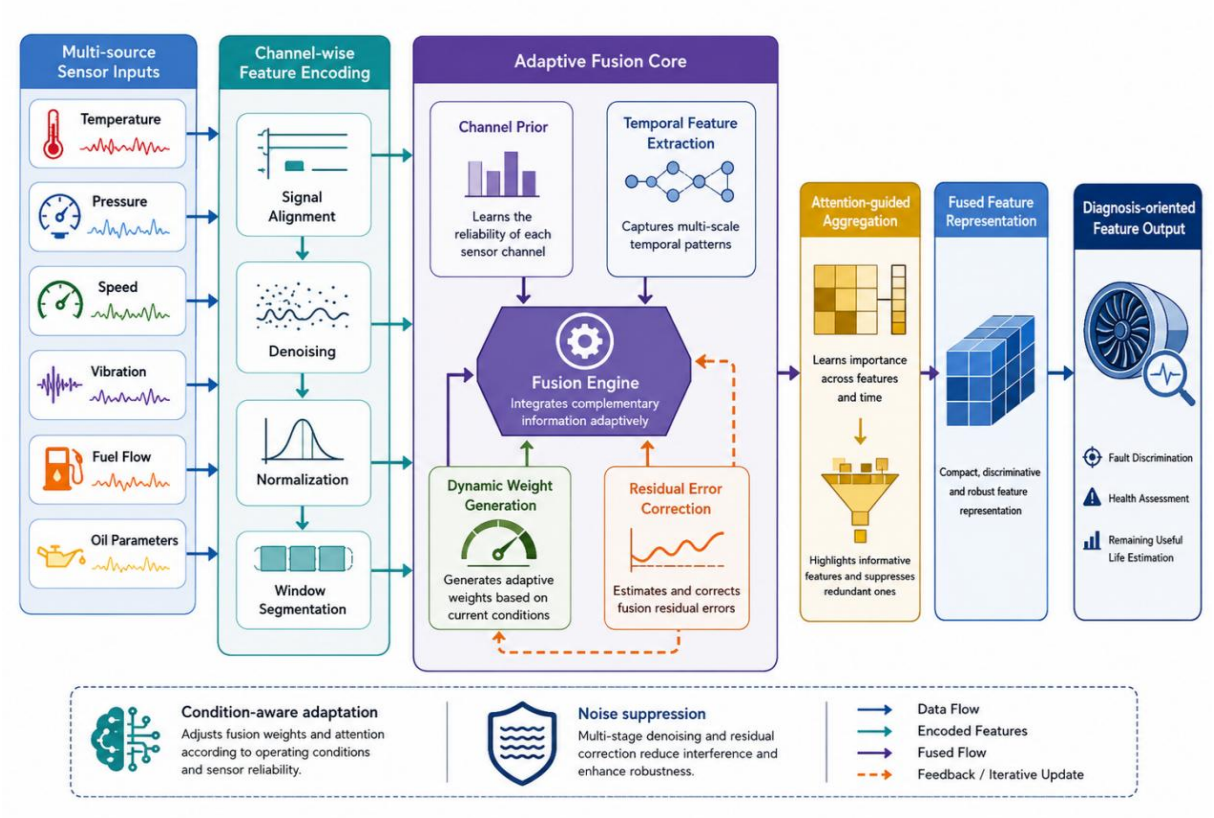

Figure 3: Structure diagram of adaptive feature fusion network

The network sends each sensor channel into the coding layer in parallel to avoid the high amplitude channel directly dominating the fusion result. Let si,m be the m-th channel sequence in the ith window, Wm be the convolution kernel parameter, bm be the bias term, and the local timing feature is expressed as follows.

$$h_{i,m}=\sigma(W_m * s_{i,m}+b_m) \tag{5}$$

where, hi,m are channel local coding results; $*$ denotes one-dimensional convolution; The $\sigma(\cdot)$ is a nonlinear activation function, which is used to extract local fluctuation, shock and trend change features.

The engine fault signal has continuous evolution characteristics, and only extracting local segments is not enough to describe the degradation trend. The gating timing unit is introduced to transfer the states before and after the window:

$$g_{i,m}=GRU(h_{i,m},g_{i-1,m}) \tag{6}$$

where, gi,m is the temporal state representation of the m-th channel; gi−1,m is the hidden state of the previous window, which is used to preserve short-time fluctuations and degradation continuity.

The weight generation layer needs to combine the channel state, the operating condition embedding, and the initial weight prior. Let qi be the embedding vector of the current working condition, $\alpha_m^{(0)}$ be the initial weight, v, Wg and Wq be the trainable parameters, and the channel score is as follows.

$$e_{i,m}=v^T \tanh\left(W_g g_{i,m}+W_q q_i\right)+\kappa\alpha_m^{(0)} \tag{7}$$

where, ei,m are channel scores; qi represents the working condition state; κ is the a priori adjustment coefficient, which is used to control the effect of the initial sensitivity on the dynamic score.

To show the difference in response of the weight generation layer at different operation stages, the thermal distribution of the fusion weights of the sensor channels is shown in Figure 4.

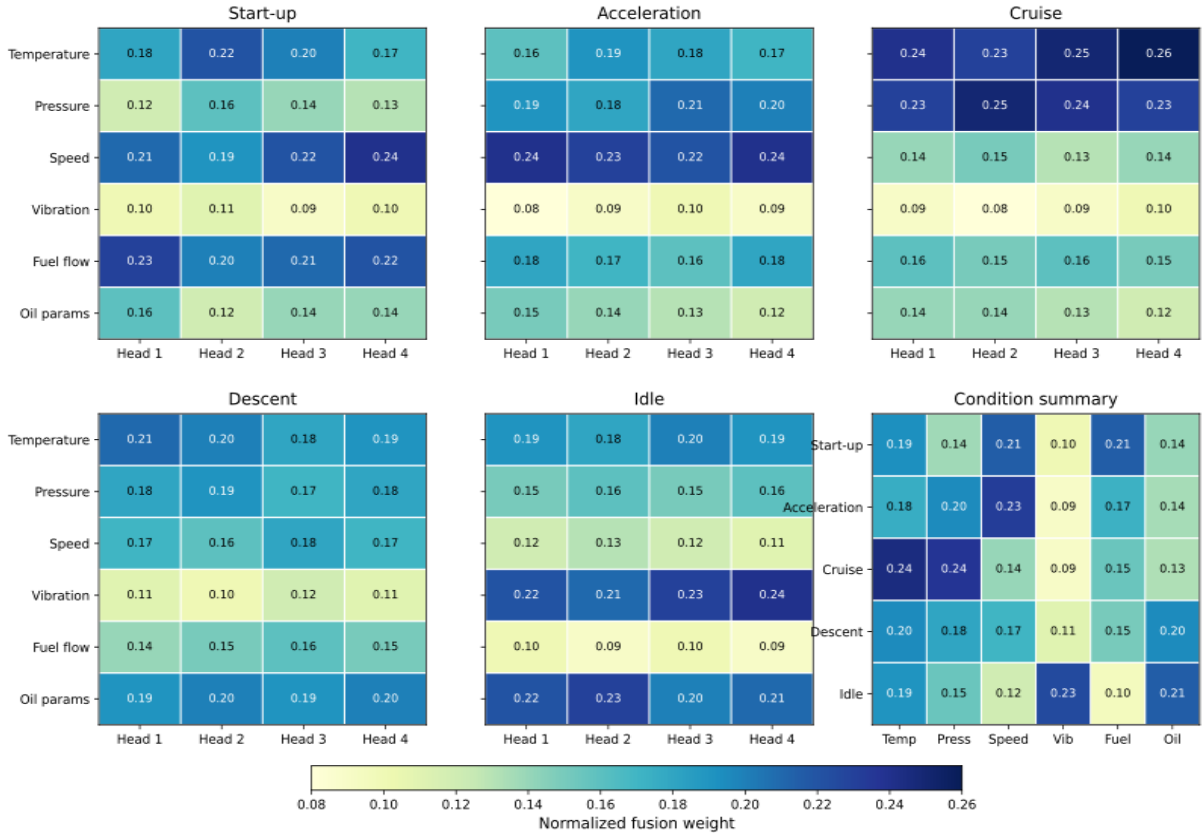

Figure 4: Heatmaps of sensor channel fusion weights under different operating conditions

The thermodynamic distribution is used to observe the adjustment of the channel contribution with changing operating conditions. The weight of temperature and pressure channels is stable in the cruise stage, and the weight of speed and fuel channel increases in the acceleration stage. The vibration channel response in the bearing abnormal samples is more prominent. Channel scores are normalized by Softmax to obtain dynamic weights:

$$\beta_{i,m}=\frac{\exp(e_{i,m})}{\sum_{j=1}^{M}\exp\left(e_{i,j}\right)} \tag{8}$$

where, βi,m is the dynamic fusion weight of the m-th class channel in the ith window. M is the total number of channels; After normalization, the sum of the weights of each channel is 1.

The weighted fusion layer compresses the channel states into unified diagnostic features, and reduces the scale offset by layer normalization:

$$F_i=LN\left(\sum_{m=1}^{M}\beta_{i,m}\,g_{i,m}\right) \tag{9}$$

where, Fi is the fused window feature; LN(·) is the layer normalization function. This feature preserves both intra-channel timing changes and cross-channel weight differences, and can be used as the input of fault classification and health status assessment.

3.3 Iterative update and error correction of the fusion algorithm

After the output Fi of the adaptive fusion layer, there may still be two types of errors. One is that the noise channel is given too high weight, which causes the fusion feature to deviate from the true fault mode. The other kind of sample distribution drift from the condition switching stage makes the same fault present different characteristic strength in different operation stages. In order to reduce such deviations, the error feedback mechanism was introduced into the fusion algorithm, and the classification prediction error was inversely acted on the feature fusion layer, and the fusion features and channel weights were iteratively corrected.

In the RTH iteration, let the true label of the ith window sample be yi, the diagnostic output probability be $\hat{p}_i^{(r)}$, and the prediction residual be defined as follows.

$$r_i^{(r)}=y_i-\hat{p}_i^{(r)} \tag{10}$$

where, $r_i^{(r)}$is the prediction residual of the r-th iteration; yi is the one-hot encoding of the true fault label; $\hat{p}_i^{(r)}$is the fault class probability output by the model. The larger the absolute value of the residual, the less adequate the fault expression of the current fusion feature for this sample.

The error correction module inputs the prediction residual and the current fusion feature into the correction mapping layer to generate the feature compensation vector:

$$\Delta F_i^{(r)}=\tanh\left(W_r r_i^{(r)}+W_f F_i^{(r)}+b_r\right) \tag{11}$$

where, $\Delta F_i^{(r)}$is the feature correction vector; $F_i^{(r)}$is the current fusion feature; Wr and Wf are trainable mapping matrices. br is the bias term; tanh(·) is used to limit the correction amplitude to avoid feature oscillation caused by error feedback.

The feature modification not only acts on the fusion vector, but also needs to adjust the channel weights. Let $d_{i,m}^{(r)}$be the contribution degree of the m-th channel in the residual, ηf and ηβ be the feature modification step and weight modification step respectively, and the update rule is as follows.

$$\begin{aligned} F_i^{(r+1)} &= F_i^{(r)}+\eta_f\Delta F_i^{(r)} \\ \beta_{i,m}^{(r+1)} &= \frac{\beta_{i,m}^{(r)}\exp(-\eta_\beta d_{i,m}^{(r)})}{\sum_{j=1}^{M}\beta_{i,j}^{(r)}\exp(-\eta_\beta d_{i,j}^{(r)})} \end{aligned} \tag{12}$$

where, $F_i^{(r+1)}$ is the modified fusion feature; $\beta_{i,m}^{(r+1)}$ is the updated channel weight. $d_{i,m}^{(r)}$ represents the contribution of the m-th channel to the current diagnostic residual, and a larger value indicates that the channel may introduce interference. M is the number of channels. This

rule is able to reduce the noise channel weight and enhance the contribution of effective fault channels.

To observe the effect of the error correction mechanism in the training process, the changes of loss, residual and validation set F1 during the iterations of the fusion algorithm can be tracked to evaluate the influence of each module on the training stability and performance, as shown in Figure 5.

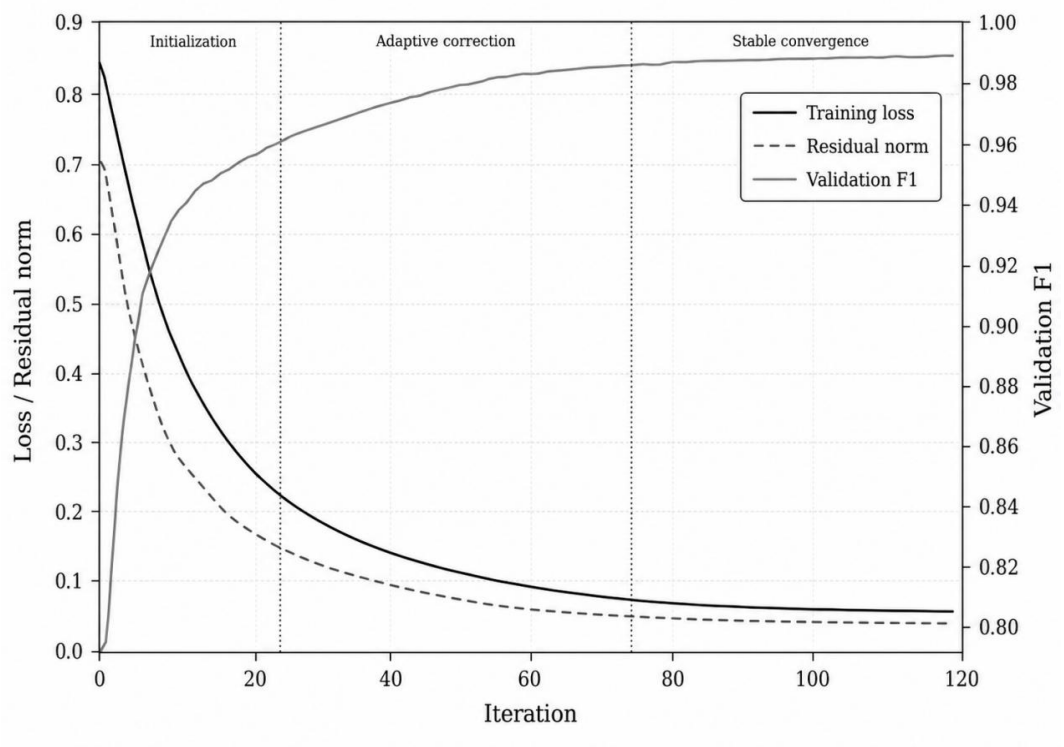

Figure 5: Graph of iterative convergence and error correction of the fusion algorithm

The curve change can be used to judge whether the model is stable and convergent. After adding error feedback, the average residual decreases faster, and the fluctuation range of F1 value in the validation set decreases, which indicates that the fusion weight update has an inhibitory effect on the working condition drift and noise interference. In order to control over-correction, the classification loss, residual constraint and weight smoothing term are used to form the convergence objective in the training process:

$$J^{(r)}=L_{ce}^{(r)}+\lambda_r\|r_i^{(r)}\|_2^2+\lambda_w\|\beta_i^{(r)}-\beta_i^{(r-1)}\|_2^2 \tag{13}$$

where, J(r) is the objective function of the r-th iteration; $L_{ce}^{(r)}$ is the cross-entropy loss for fault classification; λr is the residual constraint coefficient; λw is the weight smoothing coefficient; $\beta_i^{(r)}$ is the current channel weight vector. The training was stopped when the change of the objective function was less than the set threshold or the maximum iteration round was reached, and the stable fusion features and dynamic channel weights were finally output.

4 Fault diagnosis model construction and health management strategy module

4.1 General architecture of aero-engine fault diagnosis model

The feature FiF_iFi output by the fusion algorithm needs to be further entered into fault classification, confidence calculation, health status assessment and maintenance strategy generation modules to form executable maintenance decisions. The aero-engine fault diagnosis model adopts hierarchical structure, takes multi-source fusion features as unified input, generates fault class probability after diagnostic state mapping, and combines feature stability to judge health state.

In order to clearly show the data flow relationship between input features, model layers and policy output, the overall architecture is shown in Figure 6.

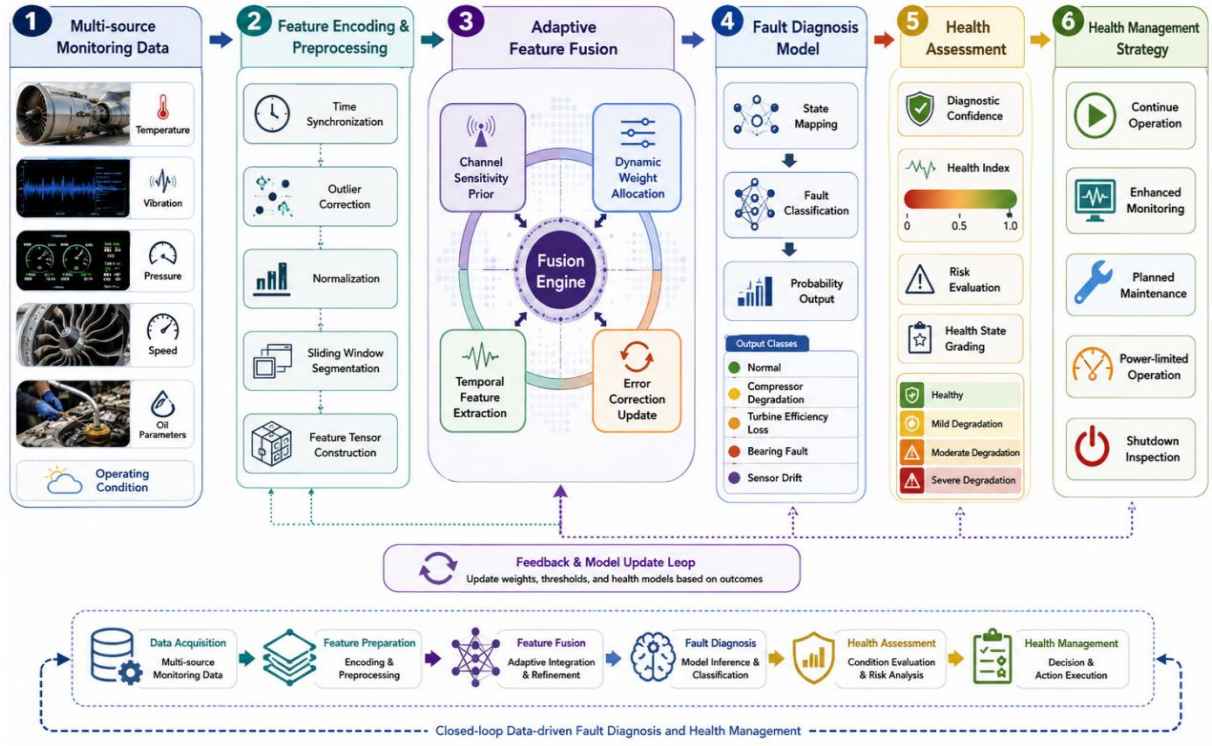

Figure 6: Overall architecture diagram of aero-engine fault diagnosis and health management

The architecture consists of five functional layers. The data fusion layer receives the channel characteristics of temperature, pressure, speed, vibration, fuel and lubric oil, and outputs the fusion vector. The diagnosis mapping layer compresses the fusion vector into the fault discrimination state. The classification layer outputs the class probabilities of normal, compressor degradation, turbine efficiency decline, bearing anomaly, sensor drift, etc. The health assessment layer calculates the confidence and health index. The policy layer generates maintenance recommendations based on risk levels. The overall mapping relationship is expressed as follows.

$$\hat{p}_i, H_i, D_i = \Phi(F_i; \Theta_e, \Theta_c, \Theta_h) \tag{14}$$

where, Fi is the fusion feature of the ith window; $\hat{p}_i$ is fault class probability vector; Hi is the

health index; Di is the maintenance decision output; Φ(·) represents the overall diagnosis and health management mapping function; Θe, Θc, Θh are parameters of diagnosis mapping layer, classification layer, and health assessment layer, respectively.

The parameters of each module of the diagnostic model need to be kept compact in structure to avoid inference delay caused by too deep network. In order to explain the implementation details of the model, Table 3 lists the main modules and parameter configurations.

Table 3: Fault diagnosis model module and parameter configuration table

Module	Input	Core Structure	Output	Main Parameters
Fusion feature input layer	Fi	LayerNorm + Dropout	Standardized features	Dropout = 0.2
Diagnostic state mapping layer	Fusion features	Fully connected layer + ReLU	State vector	Hidden layer dimension 128
Fault classification layer	State vector	Softmax classifier	Class probability	Number of classes 5
Confidence calculation layer	Probability distribution	Entropy constraint calculation	Diagnostic confidence	Temperature coefficient 1.0
Health assessment layer	Probability + state vector	Weighted scoring	Health index	Output range 0–1

In the parameter configuration, the diagnosis state mapping layer assumes the role of feature compression and class separability enhancement, the classification layer gives the fault probability, the confidence calculation layer judges the credibility of the results, and the health assessment layer transforms the diagnosis output into state variables. The mapping from fused features to diagnostic state space can be expressed as follows.

$$u_i=\mathrm{ReLU}(W_u F_i+b_u) \tag{15}$$

where, ui is the diagnosis state vector; Wu is the state mapping weight matrix; bu is the bias term; ReLU(·) is used to enhance the nonlinear discrimination ability. This state vector is used as a common input for subsequent fault classification and health assessment, so that the fault identification results can continue to serve the health management strategy generation.

4.2 Fusion feature input and fault classification recognition module

After the fused features enter the classification module, it is necessary to extract the fault expression with class discrimination ability from the continuous state vector. For example, compressor degradation will cause pressure ratio decrease and speed response hysteresis, turbine efficiency decrease will be manifested as exhaust temperature increase and fuel consumption increase, bearing anomaly is more dependent on vibration and impact characteristics. The classification module does not directly judge the fault according to the threshold of a single sensor, but uses the multi-channel correlation information in the fusion feature to output the class probability.

In order to improve the nonlinear discrimination ability of the diagnostic state vector, the hidden layer representation is composed of fully connected mapping, activation function and random inactivation. Let the diagnosis state vector obtained in the previous section be ui and the classification hidden layer output be:

$$v_i=\text{Dropout}\left(\text{ReLU}(W_c u_i+b_c)\right) \tag{16}$$

where, vi is the classification hidden layer feature; Wc is the classification mapping weight matrix; bc is the bias term; Dropout. Used to reduce the risk of overfitting. ReLU. is used to enforce nonlinear boundaries between fault classes.

The classification layer uses Softmax to output the failure probability of each class. Let the number of fault categories be (K), the classification score of the (k) fault class be oi,k, and the class probability be:

$$\hat{p}_{i,k}=\frac{\exp(o_{i,k})}{\sum_{l=1}^{K}\exp(o_{i,l})},\quad k=1,2,\ldots,K \tag{17}$$

where, $\hat{p}_{i,k}$ is the probability that the ith window belongs to the KTH type of fault. oi,k is the raw score output by the classifier; K is the total number of fault categories. A higher probability value indicates that the current fused feature matches the corresponding fault pattern to a higher degree.

To illustrate the output category, label definition and main identification basis of the classification module, Table 4 shows the mapping relationship of fault categories.

Table 4: Fault categories, output labels and identification basis table

Fault Category	Output Label	Main Sensitive Features	Identification Basis
Normal state	0	Stable fluctuations in each channel	Temperature, pressure and vibration are all within stable ranges
Compressor degradation	1	Pressure ratio change rate, speed response	Outlet pressure decreases, and speed adjustment lags
Turbine efficiency decline	2	Exhaust temperature, fuel flow	Temperature rises, and fuel consumption per unit thrust increases
Bearing abnormality	3	Vibration RMS, kurtosis, frequency band energy	Impact components are enhanced, and frequency-domain energy is concentrated
Sensor drift	4	Single-channel offset, cross-channel residual	A single variable continuously deviates, and associated channels do not match

The fault class mapping relationship is used to constrain the engineering interpretation of the classification output. The normal state samples should be characterized by multi-channel synchronous stability, the component degradation samples usually reflect the abnormal multivariate linkage, and the sensor drift is more characterized by the continuous migration of the single channel and the reduction of cross-channel correlation. The design can reduce false positives caused by single threshold judgment, and make the classification results have component directivity.

To illustrate the computational relationship between the multi-channel input, temporal coding, weight generation and fusion output of the adaptive fusion algorithm, Figure 7 shows the network structure and data flow diagram.

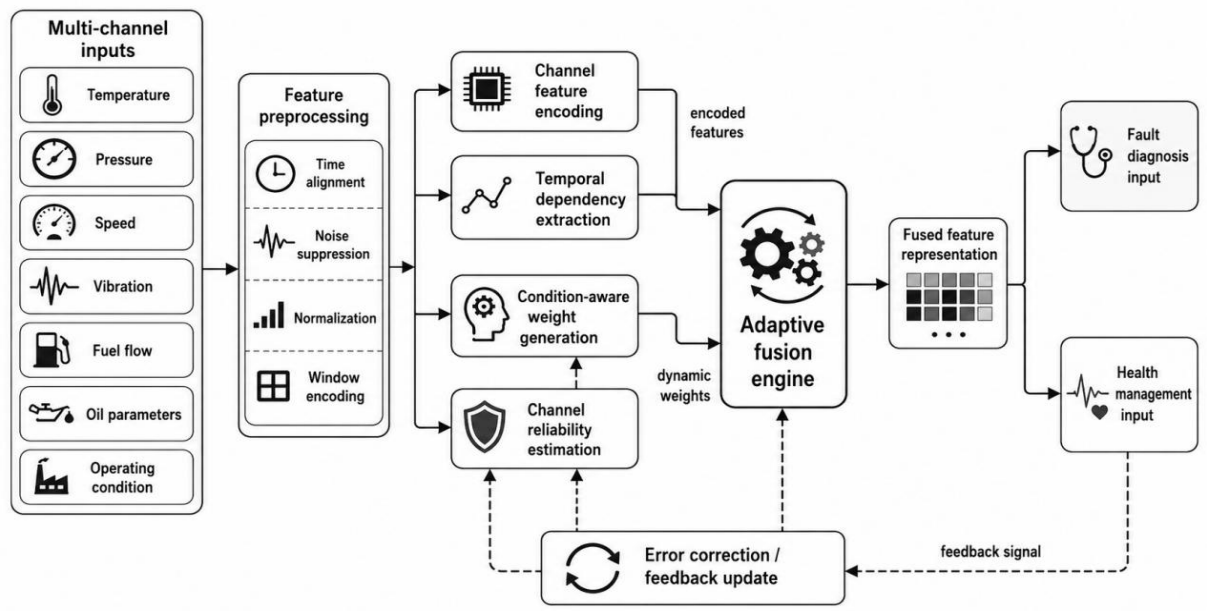

Figure 7: Schematic diagram of internal modules and data flow of the adaptive fusion algorithm

Each module completed feature coding, dynamic weight generation and fusion output in turn, providing high-quality feature input for subsequent diagnosis and health management. After preprocessing, the multi-channel input enters the channel coding, timing feature extraction and weight generation module, and the fusion feature representation is formed by the fusion engine. The error correction and feedback update module adjusts the channel weight and reliability estimation according to the output results, so as to improve the stability and adaptability of the fusion feature.

In order to solve the problem of unbalanced number of fault samples, the class weighted cross entropy loss is used for classification training. Let yi,k be the true labels, ωk be the class weights, and the loss function is as follows.

$$L_{cls}=-\frac{1}{N}\sum_{i=1}^{N}\sum_{k=1}^{K}\omega_k y_{i,k}\log(\hat{p}_{i,k}+\epsilon) \tag{18}$$

where L_{cls} is the classification loss; N is the number of training samples; yi,k are one-hot labels; ωk is used to improve the training contribution of the minority fault classes; The ϵ is the smoothing term. The loss can alleviate the class bias caused by a large number of normal samples, and improve the recognition stability of early degradation and low-frequency faults.

4.3 Diagnostic confidence calculation and health status assessment module

The output of fault classification module is the class probability, but the maximum probability does not mean that the diagnosis result is reliable. The probabilities of different classes may be close to each other in the conditions of condition switching, early degradation and multi-fault coupling of aero-engine. If the diagnosis conclusion is given only based on the maximum probability, it is easy to cause misjudgment. The confidence calculation module introduces distribution entropy constraint on the basis of class probability, which is used to judge whether the model output is centralized, stable and can be used for health assessment.

Let the class probability of the ith window sample be pi, K, the total number of fault

classes be K, the maximum value of probability be max (pi), and the diagnostic confidence is defined as follows.

$$C_i = \max(\hat{p}_i)\left(1+\frac{\sum_{k=1}^{K}\hat{p}_{i,k}\log(\hat{p}_{i,k}+\epsilon)}{\log K}\right) \tag{19}$$

where, Ci is the diagnostic confidence of the ith window; pi,k is the KTH failure probability; K is the number of classes. The ϵ is the smoothing term. The more concentrated the probability distribution, the lower the entropy value and the closer the Ci is to 1. When the probabilities of multiple classes are close to each other, the confidence decreases, indicating that the sample needs to enter the double-check or continuous observation process.

Health status assessment not only depends on the fault type, but also needs to consider the fault severity, confidence and degradation trend. Let qk be the severity coefficient corresponding to the KTH type of fault, Δi be the degradation change rate between Windows, λc and λd be the adjustment coefficients, and the health index is expressed as follows.

$$H_i = 1 - \sum_{k=1}^{K} q_k \hat{p}_{i,k} - \lambda_c(1-C_i) - \lambda_d \Delta_i \tag{120}$$

where, Hi is the health index, the higher the value is, the more stable the state is. qk is used to distinguish the degree of influence of different faults, such as bearing anomaly and turbine efficiency degradation have higher severity weight than slight sensor drift. Δi represents the decline of health status in adjacent Windows; λc and λd control the effect of insufficient confidence and degradation speed on the health index, respectively.

After the diagnosis results enter the health management link, it is also necessary to establish a continuous mapping relationship between the failure probability, diagnostic confidence, health index, risk level and maintenance strategy. Only when the classification output is further transformed into interpretable and executable state judgments, the fault diagnosis results can truly serve the operation monitoring and maintenance decision-making. Around this processing logic, the health state mapping is shown in Figure 8.

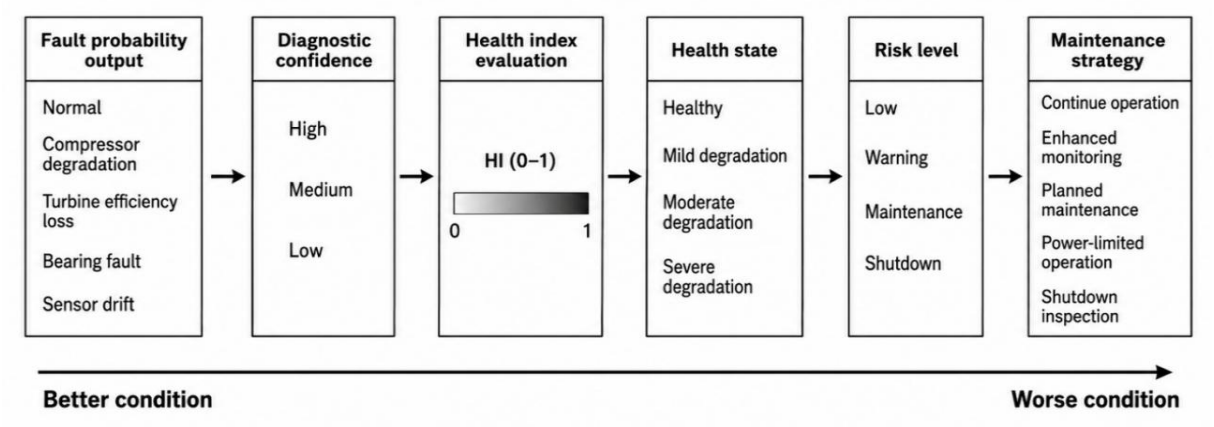

Figure 8: Failure probability -health status-maintenance policy mapping diagram

The mapping relationship transforms the classification results into health management inputs. If the fault probability is low and the confidence is high, the health index remains in the safe interval. If the failure probability increases but the confidence is insufficient, the system does not directly trigger high-level maintenance, but enters the enhanced monitoring;

If the health index decreases continuously and is accompanied by high confidence fault identification, it will enter the planned maintenance or shutdown inspection.

The risk level is determined by a combination of health index, confidence and degradation change rate. Let Ri be the risk score and ω1,ω2,ω3 be the weight coefficients, then:

$$R_i=\omega_1(1-H_i)+\omega_2(1-C_i)+\omega_3\Delta_i \tag{21}$$

where, Ri is the comprehensive risk score; 1−Hi denotes the degree of health loss; 1−Ci denotes diagnostic uncertainty; Δi represents the degree of degradation acceleration. According to the scoring interval, it can be divided into low risk, attention risk, maintenance risk and shutdown risk. The routine monitoring of low-risk samples was maintained, the sampling frequency of risk samples was increased, the maintenance risk samples were entered into the planned maintenance queue, and the shutdown risk samples were triggered for manual review and safe disposal. The confidence and health index participate in the evaluation together, which can avoid the single classification fluctuation directly affecting the maintenance decision and make the judgment of health status more stable.

4.4 Maintenance decision generation and health management strategy output module

The task of the maintenance decision module is to translate fault categories, diagnostic confidence, health indices, and risk scores into executable O&M instructions. Aero-engine health management cannot only output "normal" or "fault" labels, but also needs to give maintenance priorities, overhaul Windows, and recommendations for operation restrictions. For low-risk samples, the system maintains routine monitoring; For the samples with declining health index but insufficient confidence, encrypted sampling and manual review were entered. For high confidence fault samples, the inspection process of planned maintenance, power limited operation or shutdown is entered according to the risk degree.

Let the health index of the ith window be Hi, the diagnostic confidence be Ci, the risk score be Ri, the fault severity be $q_{\hat{k}}$, and the maintenance priority score be defined as follows.

$$P_i=\theta_1R_i+\theta_2(1-H_i)+\theta_3C_iq_{\hat{k}} \tag{22}$$

where, Pi is the maintenance priority score; Ri is the comprehensive risk score; Hi is the health index; Ci is diagnostic confidence; $q_{\hat{k}}$ is the severity coefficient corresponding to the predicted fault class $\hat{k}$; The θ1,θ2, and θ3 are the weight parameters. The higher the score, the closer the corresponding engine state of the sample is to the maintenance trigger boundary.

The overhaul window needs to be determined in combination with the risk change speed. If the health status decreases rapidly, the maintenance interval should be compressed in advance even if the current risk score has not yet reached the shutdown threshold. Let Δi be the degradation change rate, T0 be the benchmark maintenance period, and ζ be the window compression coefficient, then the proposed maintenance window is as follows.

$$T_i=\frac{T_0}{1+\zeta P_i+\Delta_i} \tag{23}$$

where, Ti is the suggested maintenance window; T0 is the baseline maintenance period; ζ is the influence coefficient of maintenance priority on maintenance cycle; Δi represents the rate of health state decline. When the maintenance priority rises or the decline of the health index accelerates, the maintenance window is shortened accordingly.

The maintenance window should also correspond to the specific risk level and policy output. In order to clarify the judgment basis of health management strategy, the health index Hi, confidence Ci and risk score Ri are divided into different intervals, and the judgment rules of maintenance strategy are shown in Table 5.

Table 5: Correspondence between intervals of health status indicators and maintenance strategies

Risk Level	Health Index Hi	Confidence Ci	Risk Score Ri	Strategy Output
Low risk	$Hi \geq 0.80$	$Ci \geq 0.70$	$Ri < 0.25$	Routine monitoring
Concern risk	$0.65 \leq Hi < 0.80$	Insufficient or fluctuating Ci	$0.25 \leq Ri < 0.45$	Increased sampling
Maintenance risk	$0.50 \leq Hi < 0.65$	$Ci \geq 0.75$	$0.45 \leq Ri < 0.70$	Planned maintenance
Shutdown risk	$Hi < 0.50$	$Ci \geq 0.80$	$Ri \geq 0.70$	Power limitation or shutdown inspection

Health index, confidence and risk score together constitute the basis of strategy decision. Maintain routine monitoring at low risk, increase sampling frequency at high risk, enter planned maintenance process at maintenance risk, and trigger power-limited operation or shutdown inspection at shutdown risk, so that health management output has clear operational boundaries.

5 Experimental verification and performance analysis

5.1 Experimental data and evaluation indicators

The experimental data are composed of open degradation sequences of turbofan engine, fault injection samples and sensor drift samples. The public degradation sequence is used to provide continuous monitoring variables such as temperature, pressure, speed and fuel flow under different operation cycles. The fault injection samples are used to supplement the categories of compressor degradation, turbine efficiency degradation and bearing anomaly. The sensor drift samples are used to test the ability of the model to identify abnormal single-channel offsets. The original variables included 21 types of sensor parameters and 3 types of working condition parameters. After time synchronization, anomaly correction, normalization and sliding window segmentation, the multi-channel timing samples that could be input into the model were formed. The window length is set to 40 time steps, the sliding step is set to 10 time steps, and each window is bound to a fault label and a health status label.

The experimental samples were divided into training set, validation set and test set according to 7:1:2. The training set is used for model parameter learning, the validation set is used to adjust the learning rate, Dropout ratio and weight smoothing coefficient, and the test set only participates in the final performance evaluation. To avoid consecutive Windows of the same engine appearing in both the training set and the test set, the data partition is done in units of engine number instead of randomly splitting by window. This reduces the risk of data leakage and is closer to the actual engine cross-individual diagnosis scenario. The main data composition is shown in Table 6.

Table 6: Experimental data set composition and fault category division table

Category Number	State Category	Number of Original Sequences/Segments	Window Samples	Training Set	Validation Set	Test Set
0	Normal state	86	3200	2240	320	640
1	Compressor degradation	64	2600	1820	260	520
2	Turbine efficiency decline	58	2400	1680	240	480
3	Bearing abnormality	42	1800	1260	180	360
4	Sensor drift	36	1500	1050	150	300
Total	—	286	11500	8050	1150	2300

The number of normal state samples in the data set is large, and the number of bearing anomaly and sensor drift samples is relatively small, which is in line with the scarcity of fault samples in actual operation and maintenance. In the training phase, the class weight is used to modify the loss function to reduce the classification bias caused by sample imbalance. The compressor degradation and turbine efficiency degradation samples are mainly used to test the recognition ability of the model for thermal performance degradation, the bearing abnormal samples are used to test the weight increase effect of the vibration channel in the fusion process, and the sensor drift samples are used to test the ability of the error correction mechanism to suppress single channel anomalies.

The evaluation metrics include Accuracy, Precision, Recall, F1-score, AUC, and average inference time. Accuracy reflects the overall classification accuracy, Precision is used to evaluate the false alarm control ability, Recall is used to evaluate the fault detection ability, F1-score is used to comprehensively measure the fault recognition effect of minority classes, AUC is used to measure the discrimination ability of multi-class probability output. The average inference time is used to determine whether the model meets the online diagnosis requirements. Considering the unbalanced class of aero-engine fault samples, macro average F1 is used as the main evaluation index, and its calculation formula is as follows.

$$F1_{macro}=\frac{1}{K}\sum_{k=1}^{K}\frac{2P_kR_k}{P_k+R_k+\varepsilon} \tag{24}$$

where, K is the number of fault categories; Pk is the accuracy rate of the KTH type of fault; Rk is the recall of the KTH type of fault; Let ε be the smoothing term. The index assigns the same weight to each type of fault, which can avoid the problem of covering up the insufficient identification of a few fault categories when the number of normal samples is large. The macro-average F1, AUC and inference time will be used to judge the model performance in the subsequent comparison experiments.

5.2 Comparative experiment and diagnostic performance analysis

The comparison experiment was completed on the same data partition, the same window length and the same test set, and the training set, validation set and test set were 8050, 1150 and 2300 window samples, respectively. The multi-channel timing window constructed in Section 5.1 was used for all model inputs, the batch size was set to 64, the maximum training round was set to 120, and the early stopping threshold was set to 15 consecutive rounds of no

F1 boost on the validation set. The optimizer uses Adam with an initial learning rate of 0.001 and a learning rate decay factor of 0.5. The comparison models include SVM, Random Forest, CNN, LSTM, CNN-bilSTM and Transformer, and the evaluation indicators are Accuracy, Precision, Recall, F1-score, AUC and average inference time.

To compare the overall performance of different models in the aeroengine fault diagnosis task, Table 7 presents the performance results of each method on the test set.

Table 7: Performance comparison table of different diagnostic models

Model	Accuracy/%	Precision/%	Recall/%	F1-score/%	AUC/%	Inference Time/ms
SVM	85.21	83.74	82.96	83.18	89.42	6.8
Random Forest	87.35	86.29	85.47	85.76	91.18	9.5
CNN	90.14	89.26	88.73	88.94	93.52	12.7
LSTM	91.08	90.41	89.86	90.03	94.11	18.6
CNN-BiLSTM	93.26	92.58	92.14	92.31	96.02	24.3
Transformer	94.05	93.46	93.01	93.19	96.48	27.9
Fusion optimization model	96.37	95.91	95.62	95.74	98.21	19.8

From the performance results, the traditional machine learning model is strongly dependent on manual statistical features, and it is difficult to fully express the continuous degradation information inside the window. The F1-score of SVM and Random Forest are 83.18% and 85.76%, respectively. CNN can extract local fluctuation and shock features, and the recognition performance is significantly improved compared with traditional methods, but it is insufficient to model long-term dependence. LSTM is superior to CNN in time series modeling, and the F1-score reaches 90.03%. CNN-BiLSTM and Transformer further improve the fault recognition ability, but the inference time is relatively increased. The F1-score and AUC of the fusion optimization model reach 95.74%and 98.21%respectively, and the inference time is controlled at 19.8 ms, indicating that the dynamic weight and error correction mechanism improve the accuracy while maintaining good online diagnosis efficiency.

After dimension reduction by UMAP, the test set samples present the spatial distribution of different fault categories, which is used to analyze the discrimination ability of the fusion features, and the results are shown in Figure 9.

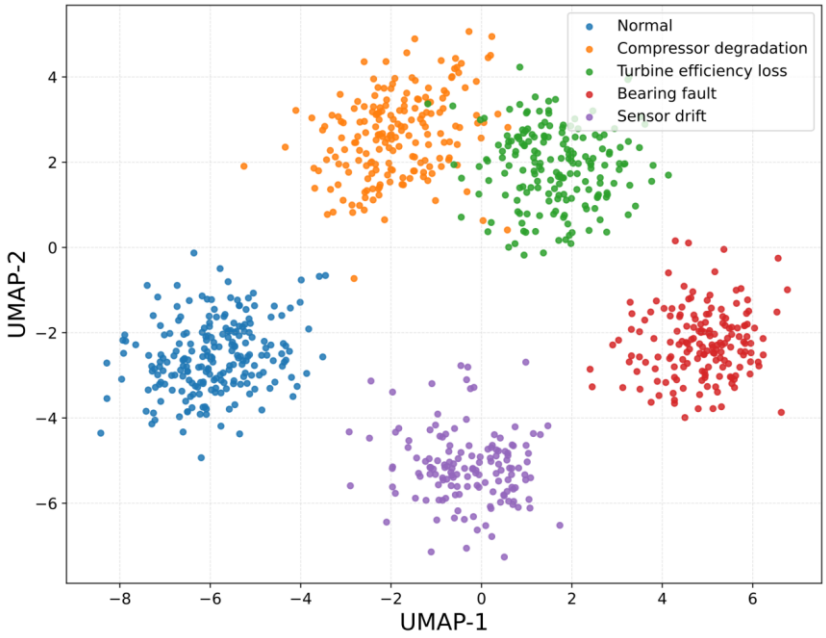

Figure 9: Visualization of fused feature dimensionality reduction clustering

The clustering results show that the normal state samples are concentrated in the lower left region, the compressor degradation samples and the turbine efficiency degradation samples have a small amount of boundary close to the central region, and the bearing abnormal samples have a clear clustering boundary due to the prominent vibration characteristics. There is a partial overlap between the sensor drift samples and the normal state samples, but the fusion model uses the cross-channel residual features to separate them from the normal samples. The results show that the adaptive fusion features not only improve the classification accuracy, but also enhance the separability of fault categories in low-dimensional space.

To evaluate the identification stability of various types of faults, the test set samples are classified and the confusion matrix is plotted, as shown in Figure 10.

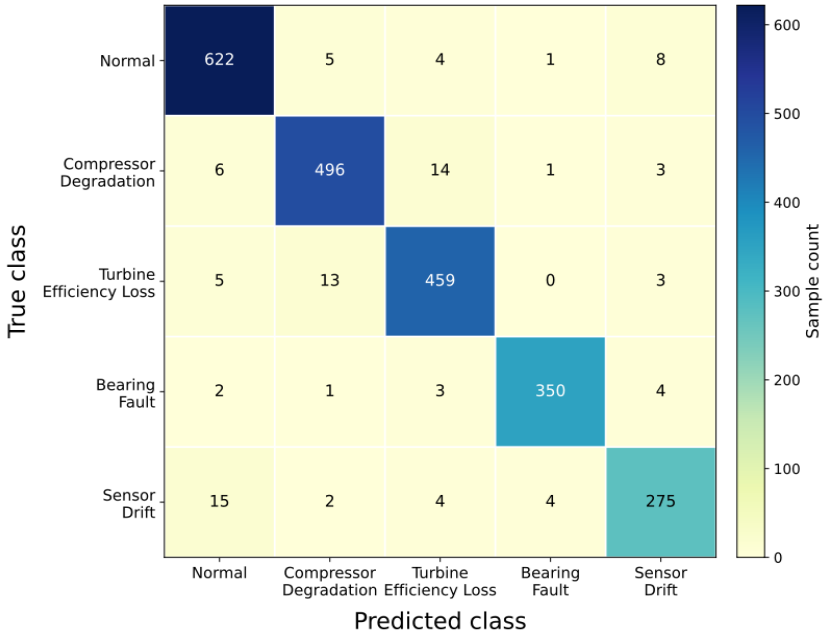

Figure 10: Heat map of confusion matrix for fault classification

The results of the confusion matrix show that 622 out of 640 test samples for normal condition are correctly identified, 496 out of 520 samples for compressor degradation are correctly identified, 459 out of 480 samples for turbine efficiency degradation are correctly identified, 350 out of 360 samples for bearing abnormality are correctly identified. Sensor drift was correctly identified in 275 out of 300 samples. The misjudgment mainly focuses on the relationship between compressor degradation and turbine efficiency degradation. Both types of faults cause changes in temperature, pressure and fuel response, and the characteristic boundaries are close in the early degradation stage. A small amount of sensor drift is misjudged as a normal state, because part of the drift amplitude is small and the cross-channel residual has not yet expanded sufficiently in a short window.

Comprehensive comparison experiments and classification results show that the advantages of the fusion optimization model mainly come from three aspects. The weight of multi-source channels can be automatically adjusted with the change of working conditions to avoid the dominant diagnosis of single channel. The error correction mechanism reduces the influence of noise channels and condition drift on the fusion features. The class-weighted loss improves the recall of minority class samples such as bearing anomalies and sensor drift. Experimental results show that the proposed model can achieve a good balance between multi-class fault recognition, weak fault separation and online reasoning efficiency.

5.3 Ablation experiment and verification of algorithm optimization effect

To verify the actual contribution of each optimization module to the diagnostic performance, ablation experiments were performed on the same test set. The complete model retained channel sensitivity prior, adaptive fusion weight, error correction, condition embedding and class weighting loss. The control group removed one of the modules separately, and the rest of the training parameters, window length, data partitioning, and optimizer Settings were kept the same. The evaluation focuses on Accuracy, F1-score, AUC, minority class recall and inference time change, avoiding using only a single accuracy to judge the quality of the model.

The specific experimental setup included five control groups: M1 removed the channel sensitivity prior, and the weights were only automatically learned by the network. M2 removed the adaptive fusion weight and used multi-channel equal-weight splicing. M3 removes the error correction module and no longer adjusts the fusion features according to the prediction residual. M4 removes the embedding of working conditions and only uses sensor features to complete the diagnosis. M5 removes the category weighting loss and uses ordinary cross-entropy training. The Accuracy of the complete model on the test set is 96.37%, F1-score is 95.74%, AUC is 98.21%, and the average inference time is 19.8 ms. The F1-score of M1 decreased to 94.86%, indicating that the sensor sensitivity prior was helpful for the model to establish a reasonable channel contribution at the early stage of training. The F1-score of M2 decreased to 93.41%, and the recall rate of bearing anomaly decreased from 97.22% to 93.61%, indicating that equal-weight fusion would weaken the role of vibration channel in bearing anomaly. The F1-score of M3 decreases to 94.05%, and the recall rate of sensor drift decreases significantly, indicating that the error correction has an inhibitory effect on single channel anomalies and noise interference. The F1-score of M4 is 94.27%, and the misjudgment between compressor degradation and turbine efficiency decline increases. The F1-score of M5 is 94.11%, and the recognition stability of minority class samples is reduced.

The ablation experiment was used to show the effect of the removal of each module on the performance of the model, and the performance degradation is shown in Figure 11.

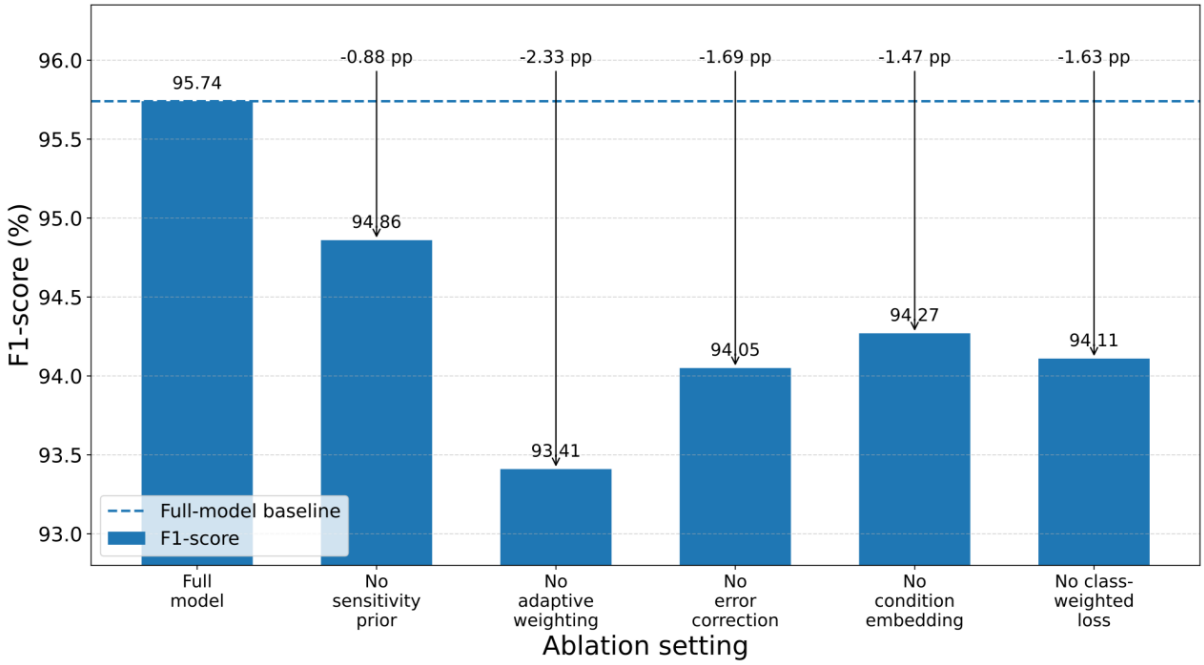

Figure 11: Waterfall plot of performance degradation in ablation experiments

From the perspective of performance degradation, the adaptive fusion weight contributes the most to the model, and the F1-score decreases by 2.33 percentage points after removal, which indicates that different sensor channels cannot be processed by fixed equal weight. The error correction module contributed the second most, with a 1.69 percentage point decrease in F1-score after removal, which mainly affected sensor drift and early degraded samples. Condition embedding is more sensitive to fault identification of thermal performance, and the confusion rate between compressor degradation and turbine efficiency degradation increases from 4.8% to 7.1% after removal. The class-weighted loss has little impact on the overall Accuracy, but has a significant impact on the recall rate of minority samples such as bearing anomaly and sensor drift, indicating that this setting is more inclined to improve the stability of fault detection.

In addition to classification performance, the health management output needs to be verified for its continuity and interpretability. An engine sequence with a decreasing trend of turbine efficiency in the test set was selected, and the continuous Windows were input into the full model to record the health index, risk threshold and maintenance strategy changes. The change curve of health index prediction and maintenance threshold formed based on this sequence can be used to reflect the transformation process of diagnosis results to health management output, as shown in Figure 12.

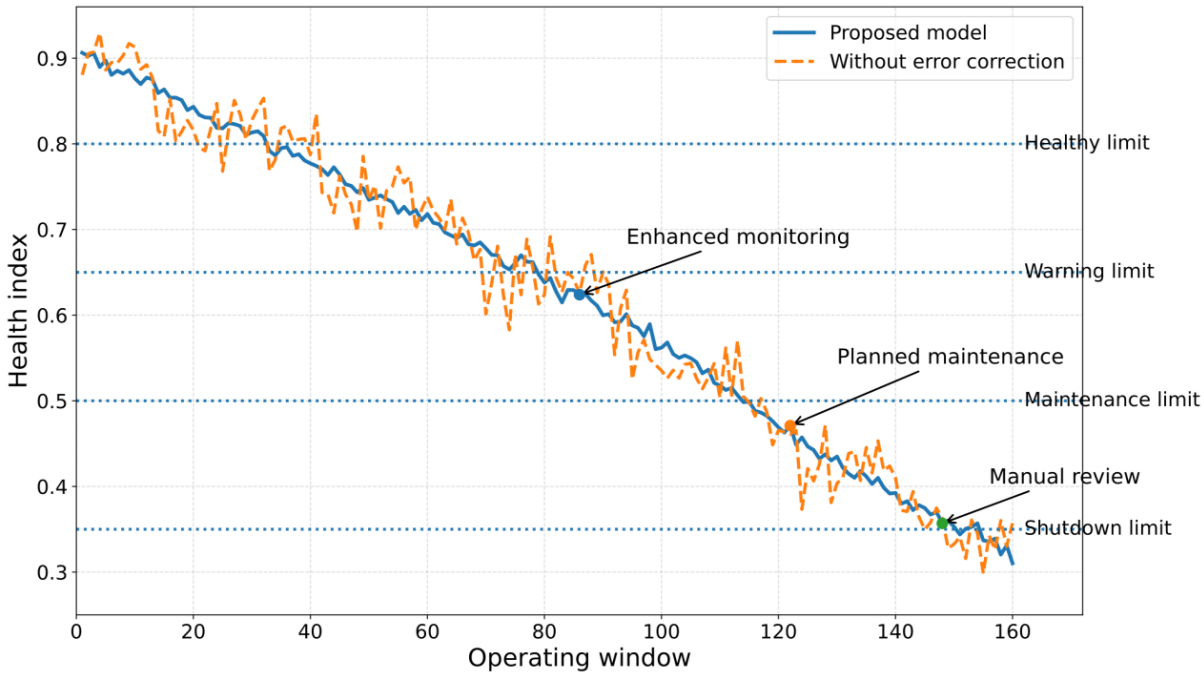

Figure 12: Health index prediction and maintenance threshold change curve

The results of the curve showed that the health index of the complete model remained above 0.82 in the first 60 Windows, and the system maintained routine monitoring. After the 85th window, the health index dropped to near 0.65, and the strategy was adjusted to encrypted sampling. After the 120th window, the health index was close to 0.50, entering the planned maintenance judgment interval. The health index near the 148th window is close to 0.35, and the system outputs recommendations for power-limited operation or shutdown inspection. After removing the error correction, the fluctuation range of the health index curve increases, and there are many short-time false triggers in the 70-95 window, which indicates that the residual feedback can reduce the influence of noise channels on the judgment of health status.

Ablation results show that channel sensitivity prior can improve the efficiency of feature selection in the early stage of training, adaptive weight can enhance the contribution of key channels, error correction can suppress noise and condition drift, condition embedding can reduce thermal performance class fault confusion, and class weighted loss can improve the recall rate of minority class faults. A consistent verification relationship was formed among the classification performance, feature fusion and health index output, indicating that the designed fusion diagnosis algorithm not only improves the fault recognition accuracy, but also can stably transfer the diagnosis results to the health status assessment and maintenance strategy generation.

6 Conclusion

The research focuses on the problem of fault diagnosis and health management under the condition of multi-source monitoring of aero-engine, and forms a continuous computing link from data preprocessing, fusion feature generation, fault recognition to maintenance strategy output. The experimental results show that the fusion optimization model keeps high recognition stability on 2300 test Windows, and the correct recognition numbers of compressor degradation, turbine efficiency decline and bearing anomaly samples reach 496,

459 and 350, respectively. Module ablation further shows that the F1-score decreases by 2.33 percentage points after the removal of adaptive weights and 1.69 percentage points after the removal of error correction, which proves that dynamic fusion and residual feedback have practical contributions to weak fault identification. In the health index verification, the 85th, 112th and 148th Windows correspond to policy changes such as encryption monitoring, planned maintenance and power limit inspection, respectively, indicating that the diagnosis results can enter the executable health management process. In the future, combined with the long-term operation data of the real fleet, the cross-model adaptation and online update ability of the model can be improved.

About the Author

Xiaolong Che was born in Harbin, Heilongjiang Province, China, in 1988. He obtained a master's degree from Harbin Engineering University, China. He is currently working at AECC South Industry Co., Ltd. and pursuing his Doctor of Engineering degree in aero-engine at Xiamen University. His main research direction is aero-engine health management.

Min Liu was born in Nanping, Fujian, China, in 1984.He graduated from Beihang University with a bachelor's degree.He is currently employed by the Optoelectronic Technology Branch of AECC South Industry Co., Ltd., and his main research direction is the development of electromechanical products.

Jiao Li was born in Shaoyang, Hunan Province, China, in 1990. She obtained a master's degree from Harbin University of Science and Technology, China. She is currently employed by the Optoelectronic Technology Branch of AECC South Industry Co., Ltd., and her main research direction is engine control system design.

References

[1] Kibrete F, Woldemichael D E, Gebremedhen H S. Multi-sensor data fusion in intelligent fault diagnosis of rotating machines: A comprehensive review[J]. Measurement, 2024, 232: 114658.

[2] engine fault diagnosis: A review[J]. Aerospace Science and Technology, 2023, 137: 108231.

[3] Sehri M, Ertugrul M, Yildirim O. Deep learning-based data fusion for intelligent fault diagnosis systems[J]. Mechanical Systems and Signal Processing, 2025, 214: 111432.

[4] Nguyen T, Medjaher K. A deep learning framework for multi-sensor fusion in fault diagnosis[J]. Information Fusion, 2024, 101: 101990.

[5] Cohen J, Huan X, Ni J. Fault prognosis of turbofan engines using deep learning approaches[J]. IEEE Transactions on Industrial Informatics, 2023, 19(8): 9123-9134.

[6] Saxena A, Goebel K. Prognostics and health management for aircraft engines: Data-driven approaches[J]. IEEE Transactions on Aerospace and Electronic Systems, 2023, 59(4): 3456-3470.

[7] un W, Wang J, Li Q. Deep neural networks for complex system fault diagnosis[J]. IEEE Transactions on Industrial Electronics, 2023, 70(6): 5921-5932.

[8] Brown M, Johnson T, Smith R. Intelligent maintenance strategies driven by fault diagnosis[J]. Journal of Intelligent Manufacturing, 2025, 36(2): 567-580.

[9] Zhang Y, Peng G, Chen X. Multimodal feature fusion for rotating machinery fault diagnosis[J]. Mechanical Systems and Signal Processing, 2024, 196: 110312.

[10] Li C, Sanchez R V, Zurita G. Multimodal deep learning for fault diagnosis: A review[J]. IEEE Transactions on Industrial Informatics, 2023, 19(5): 5503-5515.

[11] Zhou L, Wang H, Xu S. Aero-engine prognosis based on multi-scale feature fusion and multi-task learning[J]. Reliability Engineering & System Safety, 2023, 234: 109182.

[12] Garcia M, Ruiz D, Sanchez J. Data fusion strategies for industrial fault diagnosis[J]. Expert Systems with Applications, 2025, 238: 122345.

[13] Yin K, Shen Y, Chen Y. Multi-source information fusion for aero-engine fault diagnosis[J]. Applied Sciences, 2025, 15(9): 5083.

[14] Wu J, Kong L, Kang S. Aero-engine fault diagnosis using CNN-BiLSTM hybrid model[J]. Sensors, 2024, 24(3): 780.

[15] Du W, Zhang J, Meng G. Fault detection with LSTM autoencoder and attention mechanism[J]. Machines, 2024, 12(12): 879.

[16] Zhou Q, Guo Y, Wang K. Multi-head attention-based fault diagnosis method[J]. Proceedings of the Institution of Mechanical Engineers Part C, 2025, 239(21): 52983.

[17] Zhang H, Yang J. Fusion convolutional transformer for aero-engine fault diagnosis[J]. Chinese Journal of Aeronautics, 2025, 38(4): 1117-1126.

[18] Liu H, Wang Q, Li Y. Deep learning-based real-time fault diagnosis framework[J]. Reliability Engineering & System Safety, 2024, 249: 110189.

[19] Wang Y, Li X, Zhao Z. Reinforcement learning-based adaptive fault diagnosis[J]. Aerospace Science and Technology, 2024, 149: 109701.

[20] Chen B, Wang D, Li H. Adaptive feature selection and weighting for fault diagnosis[J]. Knowledge-Based Systems, 2023, 275: 110659.

[21] Garcia M, Ruiz D. Online learning for dynamic fault diagnosis systems[J]. Expert Systems with Applications, 2025, 240: 122876.

[22] Kim S, Lee J. Adaptive health monitoring using deep learning optimization[J]. IEEE Access, 2024, 12: 88921-88933.

[23] Goebel K, Saxena A. Remaining useful life prediction for aircraft engines[J]. IEEE Transactions on Reliability, 2023, 72(2): 654-666.

[24] Kim S, Lee J. Health state estimation and maintenance decision for aero-engines[J]. IEEE Access, 2024, 12: 88921-88933.